Transportation Infrastructure Precast Innovation Center (TRANS-IPIC)

University Transportation Center (UTC)

Bio-Inspired Solutions for Roadside Barriers: Exploring 3D Printing as Alternative Precast Technology — Phase II
Project N: (PU-24-RP-03)

Quarterly Progress Report
For the performance period ending *[03/31/2025]*

Submitted by:
Jan Olek[1](olek@purdue.edu),
Jeff Youngblood[2](jpyoungb@purdue.edu),
Pablo Zavattieri[1](zavattie@purdue.edu)
[1]Lyles School of Civil Engineering, Purdue University
[2]School of Materials Engineering, Purdue University

Collaborators / Partners:
Terran Robotics
Sperra (former RCAM Technology)
Circle Up Indy,Ltd
AccelNet (Arizona State University, West Pomeranian University of Technology, Poland) MS&T, UT Arlington, University of Puerto Rico)

Submitted to:
TRANS-IPIC UTC
University of Illinois Urbana-Champaign
Urbana, IL

TRANS-IPIC Quarterly Progress Report:

Project Description:

1. Research Plan - Statement of Problem

   In Phase 2 of this project, we are building upon the successful outcomes of Phase 1, where we demonstrated the potential of bioinspired architected materials through small-scale prototypes. Phase 1 revealed impressive strength, toughness, and impact resistant capabilities in these small-scale designs. In Phase 1, we also developed a cost-effective material for 3D concrete printing, comparable in price to conventional concrete, to address the economic challenges of commercial 3D printing. Now, in Phase 2, our focus will shift to scaling these bio-inspired architectures up to large scale for roadside barriers applications. We will leverage a large-scale robotic arm to precisely fabricate these expanded designs, including Bouligand and sinusoidal Bouligand (herringbone) architectures. Additionally, we will conduct thorough mechanical testing on the larger prototypes, assessing their performance under both quasi-static and dynamic loading conditions. The project was conducted on a small-scale during Phase 1. While the use of a small nozzle was beneficial for inducing more interfaces, we will also explore the use of larger nozzles and longer fibers. This has the potential to enhance mechanical performance and introduce localized anisotropy, while balancing material costs and printing time. This phase aims to validate the effectiveness of the scaled-up bioinspired designs for real-world applications, guiding final refinements and paving the way for commercialization. As we demonstrate performance at this scale, our intention is to translate these innovations toward practical industry use. A patent is currently in progress based on these findings from year 1, and we are working closely with the Purdue Office of Technology Commercialization to develop strategies for industry engagement. We are laying the groundwork to engage with companies specializing in roadside barrier systems and precast concrete technology to explore collaborative pathways for deployment. Our first step . The anticipated advancements will contribute significantly to the progress of large-scale 3D concrete printing by directly addressing key challenges associated with printing complex geometries—such as reducing print time, optimizing toolpath complexity, and enhancing the mechanical properties of printed structures, among others.

2. Research Plan - Summary of Project Activities (Tasks)

   <u>Task 1- Architected Material Designs and Fabrication</u>: Task 1 comprises four integrated subtasks aimed at adapting and scaling the 3D concrete printing process for the LSRA robotic system. Subtask 1.1 focuses on advancing toolpath design by leveraging Grasshopper to generate multi-axis, non-planar toolpaths suitable for complex geometries; if insufficient, a custom algorithm will be developed to fully exploit LSRA's capabilities. Subtask 1.2 addresses nozzle development, with the goal of creating a fork-type splitter capable of transitioning from LSRA's hose diameter to mm-scale filaments, ensuring precise, scalable, and clog-resistant material deposition. Subtask 1.3 centers on adapting the fiber-reinforced concrete mixture for large-scale printing, particularly evaluating the impact of longer fibers (10–12 mm) on printability, flowability, and structural performance. Subtask 1.4 involves a comprehensive study of printing parameters, including nozzle size, shape, and the interplay between fiber length and deposition quality, to optimize both process efficiency and mechanical outcomes in large-scale printed structures.

   <u>Task 2- Mechanical Testing</u>: We will evaluate the mechanical performance of large-scale bio-inspired architectures under quasi-static and dynamic loading conditions to validate their suitability for roadside barrier applications. Quasi-static tests will focus on assessing strength, toughness, and deformation behavior, with particular attention to compressive strength and fracture patterns. Dynamic tests, including drop-tower impact simulations, will measure impact load, energy dissipation, and crack resistance. These results will provide critical insights into the performance of the designs and guide final design refinements for commercialization.

Project Progress:

3. Progress for each research task

   <u>Task 1 Architected Material Designs and Fabrication</u>: <u>(75% completed to 3/31/2025):</u>

   <u>Task 1.1 Toolpath design</u>

As outlined in Section 2, Grasshopper—Rhino's visual programming environment was utilized for the modeling and slicing of sinusoidal Bouligand (herringbone) architectures previously investigated in Phase I. This approach enabled a parametric and highly controllable workflow for generating layered geometries. Eqn 1 defines the mathematical representation of the surface geometry of each printed layer, serving as the foundation for toolpath generation.

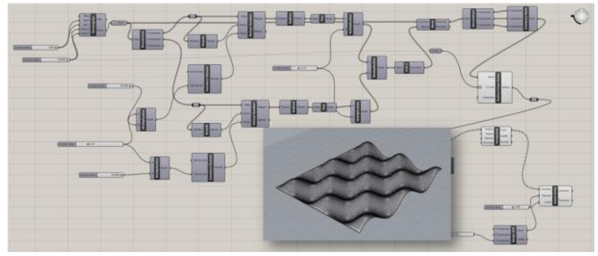

Figure 1. Grasshopper definition implemented to parametrize and slice the sinusoidal surface geometry.

$$z = A \times sin(\frac{1}{\lambda} \times x) \times sin(\frac{1}{\lambda} \times y) \qquad \text{Eqn. 1}$$

The Grasshopper environment implementation was especially useful for parametrizing the surface which enables printing at different scales and allows for varying the geometric complexity by adjusting the values of λ and A. Figure 1 shows the algorithm used in Grasshopper to parametrize and slice the surfaces and one example of the surfaces that can be generated. The Grasshopper definition (algorithm) consists of interconnected components that perform operations on data to generate parametric geometry. The resulting surface was then discretized into a set of points, which are eventually used to generate the toolpath. Grasshopper's component-based operations allow control over the number of points on the surface—effectively acting as a mesh-refinement process when converting the surface into a printable path. Figure 2 Illustrates the distribution of points over the surface and demonstrates how increasing their density enables more complex geometries and better alignment of the toolpath with specific printing parameters, such as nozzle diameter.

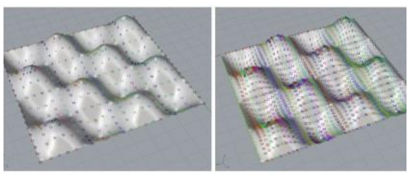

Figure 2. Point distribution over the parametrized surface used for toolpath generation. Increasing the number of points refines the mesh, enabling greater geometric complexity and improved alignment with printing parameters such as nozzle diameter.

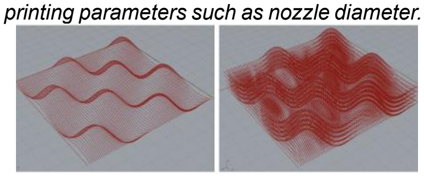

Figure 3. (a) Interpolated curves generated through surface points and connected at endpoints to form a continuous toolpath. (b) Layered array of connected curves defining the complete multi-layer toolpath for additive manufacturing.

A set of interpolated curves was generated through the discretized surface points, effectively reconstructing the desired geometry. By connecting these curves at their endpoints, a continuous toolpath is defined as illustrated in Figure 3 (a). Subsequently, an array of these connected curves is replicated in the vertical direction to construct the layered toolpath sequence, as shown in Figure 3 (b). Following the generation of the toolpath in the Rhino environment, the RhinoRobot plugin is employed to convert the geometry into RAPID code, enabling large-scale additive manufacturing with the ABB IRB6700 robotic arm. Figure 4 illustrates the integration of the generated surface within the simulated environment of the ABB IRB6700 robotic arm`. This visualization demonstrates how the toolpath conforms to the intended geometry while accounting for the robotic arm's kinematic constraints and workspace. Integration allows for verification of reachability, orientation, and collision-free movement prior to physical fabrication.

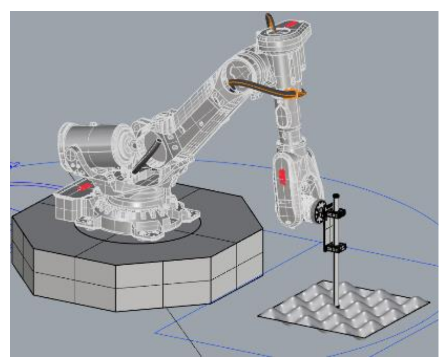

Figure 4. Integration of the generated surface and toolpath within the ABB IRB6700 robotic arm environment.

Task 1.2 Nozzle development:

During the first quarter, key factors influencing nozzle design were identified and analyzed to ensure uniform flow distribution and optimal print quality. These included flow distribution and manifold design, dynamic nozzle geometry adaptation, material rheology and compatibility (Task 1.3), and critical printing process parameters (Task 1.4). A comprehensive literature review was conducted to examine how these challenges have been addressed across various industries, providing valuable insights to inform the development of the multi-outlet extrusion system.

Please note that for the surface defined by equation 1, any intersection with a plane perpendicular to the ground plane (x-y) results in a 2D sinusoidal wave projection. To accurately print this geometry, the nozzle's outlets must dynamically conform to the evolving sinusoidal shape as the printing progresses. This requires the nozzle to adapt its geometry in real-time to match the desired sinusoidal pattern, ensuring precise material deposition and structural integrity of the printed object.

In extrusion-based additive manufacturing, particularly in 3D concrete printing, the design of a shapeshifting, fork-type nozzle necessitates meticulous attention to flow distribution across all outlets to ensure optimal printing outcomes. The dynamic alteration of the nozzle's outlets disposition during printing introduces complexities in maintaining uniform material flow. Uneven flow can lead to inconsistencies in layer deposition, compromising the structural integrity and surface quality of the printed object.

The needle valve mechanism presented by Morita et al. has been identified as a relevant and potentially adaptable solution for flow control in multi-outlet extrusion systems [1]. Their design employs a vertically actuated needle to regulate material flow in fused granular fabrication, enabling precise, slicer-integrated retraction and deposition control. De Vries et.al investigated the pressure drop behavior in material extrusion additive manufacturing, introduced a novel nozzle design incorporating a pin inserted through the side of the nozzle in direct contact with the molten polymer [2]. The force exerted by the melt on the pin is transmitted to an external Wheatstone bridge load cell, enabling calculation of the nozzle pressure drop. This concept can be combined with the needle valve mechanism to control the flow at each outlet in real time, the electronic signal coming from a load cell in can be used to control the needle valve mechanism through a PID circuit. Calculations related to nozzle dimensions, geometry, and material selection will be conducted in alignment with the findings from Task 1.4.

Task 1.3 Mixture development:

The focus in this first quarter was to determine the optimal fiber content for 3D printed concrete which is usually the maximum fiber dosage that still allows good flow and extrusion. Compiling recent studies in Table 2, this optimal point tends to be around 0.5%–1% by volume for many common fibers.

It is also to be noted that because of particle movement, the flow of printed concrete through a pipe is separated into two layers: the lubrication layer and the bulk concrete. Both layers have distinct rheology, and the total yield stress and plastic viscosity of the two layers determine how much pumping is needed for a printable concrete mix. Studies show varying the aggregate-binder ratio from 1.0 to 1.4 and 1.8 and observed that pumping requirements increased from 9 to 12 bar and 17 bar, respectively, which shows that increasing the aggregate content shall increase the pressure required for pumping printable concrete [3]. Overall, successful scaling from laboratory conditions to practical LSRA applications will be targeted with the optimized nozzle.

Task 1.4 Printing parameter study progress:

In the field of 3D concrete printing, the design and selection of nozzle sizes, shapes, geometries and printing parameters are critical parameters that influence printability, quality, and performance of printed structures. A thorough literature review was conducted to identify key trends and findings related to how variations in these parameters affect the rheological properties of the concrete mix and have implications for bonding strength and structural integrity of the final product.

(1) Nozzle Size: The size of the nozzle directly affects the extrusion rate and the overall print quality. Smaller nozzle diameters, such as the ultra-thin 6 mm nozzle, have been shown to enhance the detail and accuracy of the printed structures [4]. Larger nozzle diameters are reported to increase the flow rate of the concrete mix but can result in thicker extrusions, potentially leading to imperfections such as uneven surfaces or weak inter-layer adhesion [5], [6]. Table 1 summarizes these parameters employed in previous studies [5], [7], [8], [9], [10], [11]. These parameters vary widely due to the absence of a standardized guideline for setting print parameters across different types of printable materials.

(2) Nozzle Shape and Geometry: The design affects extrudability and layer shape, with circular nozzles better for complex geometries [13], [14], some researchers have also used rectangular nozzles due to fewer gaps [8], [12]. The shape of the nozzle also plays an essential role in shaping the extrudate

and the bond between layers. Different nozzle designs, such as circular versus flat, yield varied outcomes in terms of material deposition and fiber orientation, which affect the structural integrity and aesthetic properties of the printed object [15]. Studies emphasize that nozzle geometries can be tailored to enhance bonding between layers during the printing process, significantly affecting the mechanical performance of the final product [16], [17]. Moreover, optimized nozzle geometries contribute to achieving desired surface finishes and minimizing voids, which are critical elements in load-bearing concrete structures [18].

Table 1 Print parameters and nozzle features

References	Nozzle orifice shape	Nozzle size (mm)	Extrusion velocity (L/min)	Printing speed (mm/s)	Nozzle lift height (mm)
[8]	Rectangular	30*20	1.6	44	20
[12]	Rectangular	10*20	3	150	—
[9]	Circular	10	0.5	80	—
[10]	Circular	9	—	—	6
[11]	Circular	25	—	20	20
[7]	Slice	—	—	60	25.4-38.1

(3) Extrusion Rates and Printing Parameters: The extrusion mechanism provides extrusion driving forces for concrete extrusion. It describes how fresh cementitious paste is extruded from the extruder entry towards the outlet exit [19]. There are three types of extruder mechanisms: primary motivation [20], ram extrusion; and screw extrusion. To optimize material flow during extrusion, some researchers have used tapered chamber nozzles that gradually reduce the cross-sectional area, helping to control the flow and maintain a consistent rate [21], [22]. Another benefit of the conical shape is that it prevents dead zones near the outlet, reducing the risk of clogging and improving extrusion quality [23].
Synchronizing nozzle velocity with the extrusion rate is essential to ensure print quality, as any mismatch can cause defects like uneven layer thickness or poor bonding, weakening the printed structure [24]. Processing parameters such as nozzle height and standoff distance also play a key role; maintaining the right distance supports steady material flow and proper layer adhesion [25]. These parameters must be carefully controlled, as they significantly influence the fresh properties and buildability of extruded concrete [26], [27]. Nan et al. [5] developed theoretical models showing that reducing extrusion velocity and nozzle length lowers resistance, and their results indicate that slower printing speeds allow for thicker layers, while layer width increases linearly with extrusion velocity regardless of speed. Overall, the literature suggests that careful consideration of nozzle size, shape, and operational parameters is crucial for the advancement of 3D concrete printing technology. To ensure dimensional consistency and avoid surface defects, the nozzle lift height should equal the layer thickness.

<u>Task 2 Mechanical Testing</u>: (0% completed). Task 2.1 (and subsequent sub-tasks) are scheduled to start in month 6 (see below).

4. Percent of research project completed

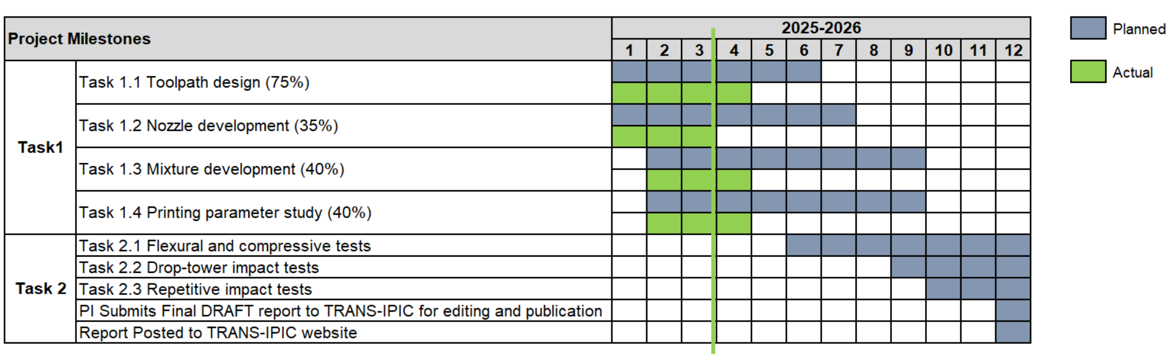

5. Expected progress for next quarter

The work for Task 1.1 will involve the optimization of the current tool path to eliminate unnecessary tool movements and avoid potential collisions with the printed object. This includes developing a method to process the discretized points over the surface, enabling the generation of multiple sets of interpolated curves with specific user-defined orientations. Additionally, the task will include the testing of the resulting toolpath on the robotic arm to validate motion planning and ensure that the nozzle follows the intended trajectory without interference.

The work planned for Task 1.2 will focus on applying findings from the literature review to a CAD design of the nozzle. This includes incorporating internally proposed mechanisms that allow the nozzle outlets to evolve into a sinusoidal shape throughout the printing process. The task will also involve designing and integrating control systems for actuating each outlet's movement along the z-axis, as well as implementing flow control mechanisms. A PID controller will be developed and tested to regulate the needle valve system, ensuring precise and synchronized material extrusion from each outlet.

For task 1.3 several concrete mixture designs will be studied incorporating different fibers for 10- and 12-mm lengths. Studies will be conducted to observe the change of rheological parameters in function of fiber lengths. Subsequently, a series of printability trials will be conducted using the LSRA printer, emphasizing the compatibility of larger nozzle sizes and the feasibility of complex, non-planar printing paths. This phase will involve iterative adjustments to fiber length, dosage, and mixture proportions based on continuous feedback and printability outcomes.

In parallel, systematic mechanical testing (Task 2), including tensile, flexural, and compressive strength assessments, will be performed to confirm that mechanical integrity remains consistent with targets set during Phase 1. Results from these combined tests will guide further refinement of the mixture and printing parameters, aiming to optimize overall performance, minimize waste, and maintain sustainability objectives. Effective documentation of each iteration will support data-driven decisions, facilitating a smooth transition to practical application and ensuring reproducibility and scalability in larger-scale fabrication scenarios.

Next quarter for tasks 1.4 involves a more comprehensive study that plans to investigate the effects of extrusion velocity, printing speed, and nozzle lift height on extrusion and deposition. An exact printing parameter will be determined to better control filament placement and enhance local anisotropy and overall structural performance.

6. Educational outreach and workforce development:

The team hosted a seminar titled "Autonomous Earthen Construction and Terran Robotics First Permitted Home" (03/07/25), delivered by Daniel Weddle, Chief Design Officer at Terran Robotics, as part of ongoing efforts to expose students and faculty to innovative construction technologies. Additionally, the team is preparing new materials to offer CE 497 – 3D Printing for Infrastructure Applications during the Fall 2025 semester

Purdue Engineering Distinguished Lecture Series – (September 12th) Description: The Concrete 3D Printing Team presented a poster featuring their latest work, in which research from TRANS-IPIC was highlighted. The poster emphasized Purdue's efforts to advance sustainable and resilient infrastructure through innovative 3D printing technologies.

7. Technology Transfer

Provisional Patent Applications submitted (Purdue Office of Technology Commercialization)

- Youngblood, J. P., Olek, J., Zavattieri, P. D., Wang, Y., Douba, E. A., Low Carbon, Low Cost Cement Mix Containing Cellulose Nano Fiber and Limestone Filler For 3D Concrete Printing, (Available for License)
- Zavattieri, P. D., Youngblood, J. P., Olek, J., Wang, Y., Energy-Absorbing Roadside Barriers Using Bio-Inspired Architecture and 3D Concrete Printing (Available for License)
- Zavattieri, P. D., Youngblood, J. P., Olek, J., Wang, Y., Cubillos, L. David, Reconfigurable acoustic metamaterials for traffic noise reduction (Available for License)
- Zavattieri, P. D., Olek, J., Marika Santagata, Youngblood, J. P., Wang, Y., Hygrolock - reinforcement for building blocks made of earth materials (Available for License)

Research Contribution:

8. Papers that include TRANS-IPIC UTC in the acknowledgments section:

   - *Y. Wang, A.E. Douba, J. Olek, P. D. Zavattieri,J.P. Youngblood, Better, Cheaper, Greener: A high-performance Cementitious Composite for Sustainable Concrete 3D Printing, to be submitted to Nature Communications.*
   - *Y. Wang, L. Shyamsunder J. Olek, P. D. Zavattieri, J.P. Youngblood, Impact resistant sinusoidally-architected Bouligand 3DPC materials inspired by the mantis shrimp, to be submitted to Advanced Materials.*

9. Presentations and Posters of TRANS-IPIC funded research:

   - Delivered the talk titled 'Bio-Inspired Solutions for Roadside Barriers: Exploring 3D Printing as an Alternative Precast Technology' at the TRANS-IPIC Research Highlights Webinar on February 19, 2025, as part of the project's dissemination efforts.

10. Please list any other events or activities that highlights the work of TRANS-IPIC occurring at your university (please include any pictures or figures you may have). Similarly, please list any references to TRANS-IPIC in the news or interviews from your research.

Purdue CCE Impact Magazine: Purdue University's recent research highlights significant advancements in 3D-printed construction. Collaborating with Terran Robotics, Purdue engineers are developing sustainable and affordable housing solutions by integrating artificial intelligence with 3D printing technologies. The team is experimenting with 'cob,' a low-carbon material composed of clay, sand, water, and straw, aiming to optimize its strength and resilience for construction applications. This initiative not only addresses environmental concerns but also offers innovative approaches to modern housing challenges.
https://engineering.purdue.edu/CCE/Media/Impact/2025-Spring/building-the-future

Appendix 1: Research Activities, leadership, and awards (cumulative, since the start of the project)

A. Number of presentations at academic and industry conferences and workshops of UTC findings
   - No. = 1 (in 2025, for phase II)

B. Number of peer-reviewed publications submitted based on outcomes of UTC funded projects
   - 2 papers to be submitted that include an acknowledgement of TRAN-IPIC.

C. Number of peer-reviewed journal articles published by faculty.
   D. 2 papers to be submitted that include an acknowledgement of TRAN-IPIC.

E. Number of peer-reviewed conference papers published by faculty.
   - No. = 0

F. Number of TRANS-IPIC sponsored thesis or dissertations at the MS and PhD levels.
   - No. MS thesis = 0
   - No. PhD dissertations = 1 (Dec. 2024)
   - No. citations of each of the above = 0 (the PhD thesis has not been published yet)

G. Number of research tools (lab equipment, models, software, test processes, etc.) developed as part of TRANS-IPIC sponsored research
   - Research Tool #1 (Toolpath development) = Parametric Toolpath Generation Model for Non-Planar 3D Printing, a computational model developed in Grasshopper for generating toolpaths tailored to non-planar, multi-axis 3D concrete printing. The model allows users to define sinusoidal surface geometries, discretize them into point sets, and create interpolated curves that serve as custom toolpaths for robotic extrusion. This tool supports real-time geometry adjustments and can be adapted to different nozzle configurations and print parameters. Link available upon request.

H. Number of transportation-related professional and service organization committees that TRANS-IPIC faculty researchers participate in or lead.
   - Professional societies
     - No. participated in =1
     - No. lead = 1
   - Advisory committees (No. participated in & No. led)
     - No. participated in = 1
     - No. lead = 0
   - Conference Organizing Committees (No. participated in & No. led)
     - No. participated in = 2
     - No. lead = 1
   - Editorial board of journals (No. participated in & No. led)
     - No. participated in = 2
     - No. lead = 0
   - TRB committees (No. participated in & No. led)
     - No. participated in =1
     - No. lead = 0

I. Number of relevant awards received during the grant year
   - No. awards received = 1

J. Number of transportation related classes developed or modified as a result of TRANS-IPIC funding.
- No. Undergraduate = 1
- No. Graduate = 1

K. Number of internships and full-time positions secured in the industry and government during the grant year.
- No. of internships = 0
- No. of full-time positions = 1

Appendix 2:

Table 2 Fiber Type vs. Volume Fraction and Flowability in 3D Printed Concrete

Fiber Type	Volume Fraction	Flowability Impact	Optimal Content
Steel fibers	0.25 % to 1% ([28])	Slump flow decreases with fiber content (few % drop at 0.5% vol). Minimal rheology change at very low dosages; <5% slump reduction up to ~1% observed in one review. ([29])	Heavy, stiff fibers; lowest impact on slump among fiber types. Often kept ⩽1% for smooth extrusion. >1% can cause nozzle clogging or rough prints.
Polypropylene	0.25 to 2% ([29])	Increases yield stress notably; each 0.5% increment stiffens mix. Viscosity rises with fiber content. High dosages (≥1.5%) can cause severe flow loss (poor extrusion). (([28])	Improves buildability at moderate content but too much causes filament breakage. Optimal ~0.5–1.0% vol in many studies for balanced workability and strength. Longer PP fibers exacerbate flow issues more than short fibers. (([28])
Glass Fibers	0.2 to 0.6% ([29])	Slightly reduces flow at higher end (e.g. 0.5% vol caused <10% slump diameter drop). At very low content, can even increase flow (0.2% gave 9% higher slump flow vs. no fiber). ([29])	Moderate-length glass fibers are relatively benign to mix flow at <0.5%. Commonly used ~0.5% vol to boost tensile strength with minimal print issues. Good for improving interlayer bonding and strength with little workability penalty at low dosage. ([29])
Basalt Fibers	0.2 to 0.85% ([29])	**Minimal impact on slump** – under 5% reduction even at ~0.8% vol. Behaves similar to steel fiber in not greatly altering slump flow for given content. ([29])	Used up to ~0.8% vol without much flowability loss. Tends to improve buildability slightly (fiber network helps stability). A good balance is ~0.5% vol for added ductility with little loss of flow. ([29])
Polyvinyl Alcohol	0.5 to 2% ([29])	Greatly increases mix viscosity, causing significant slump flow reduction (up to 25–30% less slump at ~1.5% vol). Workability drops sharply as content rises. ([29])	Requires high paste content and admixture to print. For normal 3DPC, PVA is usually kept ⩽0.5–1.0% to avoid pumpability issues. Very effective at bridging cracks, but limit to low % for flow. ([28], [29])
Carbon Fibers	0.5 to 1.5% ([29], [30])	Moderate flow impact: fine carbon filaments (e.g. 6 mm) caused only ~5% slump reduction at 0.5% vol. Higher content makes mix stickier; e.g. required higher extrusion pressure even at 0.5%. ([29], [30])	Often used in micro-fiber form. ~1.0–1.5% vol is a recommended upper range for printability. ([30])

References:

[1] L. Morita, A. Asad, X. Sun, M. Ali, and D. Sameoto, “Integration of a needle valve mechanism with cura slicing software for improved retraction in pellet-based material extrusion,” *Addit. Manuf.*, vol. 82, p. 104045, Feb. 2024, doi: 10.1016/j.addma.2024.104045.

[2] S. De Vries, T. Schuller, F. J. Galindo-Rosales, and P. Fanzio, “Pressure drop non-linearities in material extrusion additive manufacturing: A novel approach for pressure monitoring and numerical modeling,” *Addit. Manuf.*, vol. 80, p. 103966, Jan. 2024, doi: 10.1016/j.addma.2024.103966.

[3] M. K. Mohan, A. V. Rahul, K. Van Tittelboom, and G. De Schutter, “Evaluating the Influence of Aggregate Content on Pumpability of 3D Printable Concrete,” in *Second RILEM International Conference on Concrete and Digital Fabrication*, F. P. Bos, S. S. Lucas, R. J. M. Wolfs, and T. A. M. Salet, Eds., Cham: Springer International Publishing, 2020, pp. 333–341. doi: 10.1007/978-3-030-49916-7_34.

[4] L. He, J. Z. M. Tan, W. T. Chow, H. Li, and J. Pan, “Design of novel nozzles for higher interlayer strength of 3D printed cement paste,” *Addit. Manuf.*, vol. 48, p. 102452, Dec. 2021, doi: 10.1016/j.addma.2021.102452.

[5] N. Zhang and J. Sanjayan, “Extrusion nozzle design and print parameter selections for 3D concrete printing,” *Cem. Concr. Compos.*, vol. 137, p. 104939, Mar. 2023, doi: 10.1016/j.cemconcomp.2023.104939.

[6] M. David, N. Freund, K. Dröder, and D. Lowke, “The effects of nozzle diameter and length on the resulting strand properties for shotcrete 3D printing,” *Mater. Struct.*, vol. 56, no. 8, p. 157, Oct. 2023, doi: 10.1617/s11527-023-02246-1.

[7] A. Kazemian, X. Yuan, E. Cochran, and B. Khoshnevis, “Cementitious materials for construction-scale 3D printing: Laboratory testing of fresh printing mixture,” *Constr. Build. Mater.*, vol. 145, pp. 639–647, Aug. 2017, doi: 10.1016/j.conbuildmat.2017.04.015.

[8] A. V. Rahul, M. Santhanam, H. Meena, and Z. Ghani, “3D printable concrete: Mixture design and test methods,” *Cem. Concr. Compos.*, vol. 97, pp. 13–23, Mar. 2019, doi: 10.1016/j.cemconcomp.2018.12.014.

[9] B. Panda, C. Unluer, and M. J. Tan, “Investigation of the rheology and strength of geopolymer mixtures for extrusion-based 3D printing,” *Cem. Concr. Compos.*, vol. 94, pp. 307–314, Nov. 2018, doi: 10.1016/j.cemconcomp.2018.10.002.

[10] T. T. Le, S. A. Austin, S. Lim, R. A. Buswell, A. G. F. Gibb, and T. Thorpe, “Mix design and fresh properties for high-performance printing concrete,” *Mater. Struct.*, vol. 45, no. 8, pp. 1221–1232, Aug. 2012, doi: 10.1617/s11527-012-9828-z.

[11] D. Asprone, F. Auricchio, C. Menna, and V. Mercuri, “3D printing of reinforced concrete elements: Technology and design approach,” *Constr. Build. Mater.*, vol. 165, pp. 218–231, Mar. 2018, doi: 10.1016/j.conbuildmat.2018.01.018.

[12] S. C. Paul, Y. W. D. Tay, B. Panda, and M. J. Tan, “Fresh and hardened properties of 3D printable cementitious materials for building and construction,” *Arch. Civ. Mech. Eng.*, vol. 18, no. 1, pp. 311–319, Jan. 2018, doi: 10.1016/j.acme.2017.02.008.

[13] F. Lyu, D. Zhao, X. Hou, L. Sun, and Q. Zhang, “Overview of the Development of 3D-Printing Concrete: A Review,” *Appl. Sci.*, vol. 11, no. 21, p. 9822, Oct. 2021, doi: 10.3390/app11219822.

[14] H. Chen, D. Zhang, P. Chen, N. Li, and A. Perrot, “A Review of the Extruder System Design for Large-Scale Extrusion-Based 3D Concrete Printing,” *Materials*, vol. 16, no. 7, p. 2661, Mar. 2023, doi: 10.3390/ma16072661.

[15] T. Kim, R. Trangkanukulkij, and W. S. Kim, “Nozzle shape guided filler orientation in 3D printed photo-curable nanocomposites,” *Sci. Rep.*, vol. 8, no. 1, p. 3805, 2018.

[16] H. G. Şahin and A. Mardani, “Mechanical properties, durability performance and interlayer adhesion of 3DPC mixtures: A state-of-the-art review,” *Struct. Concrete*, vol. 24, no. 4, pp. 5481–5505, Aug. 2023, doi: 10.1002/suco.202200473.

[17] B. Liu and L. Wang, “Research progress on constructability of 3D printed concrete,” in *Journal of Physics: Conference Series*, IOP Publishing, 2024, p. 012048. Accessed: Mar. 25, 2025. [Online]. Available: https://iopscience.iop.org/article/10.1088/1742-6596/2853/1/012048/meta
[18] W. Lao, M. Li, L. Masia, and M. J. Tan, “Approaching rectangular extrudate in 3D printing for building and construction by experimental iteration of nozzle design,” 2017, Accessed: Mar. 25, 2025. [Online]. Available: https://dr.ntu.edu.sg/handle/10220/44502
[19] A. Perrot, D. Rangeard, V. N. Nerella, and V. Mechtcherine, “Extrusion of cement-based materials - an overview,” *RILEM Tech. Lett.*, vol. 3, pp. 91–97, Feb. 2019, doi: 10.21809/rilemtechlett.2018.75.
[20] V. Mechtcherine *et al.*, “Extrusion-based additive manufacturing with cement-based materials – Production steps, processes, and their underlying physics: A review,” *Cem. Concr. Res.*, vol. 132, p. 106037, Jun. 2020, doi: 10.1016/j.cemconres.2020.106037.
[21] V. Nienhaus, K. Smith, D. Spiehl, and E. Dörsam, “Investigations on nozzle geometry in fused filament fabrication,” *Addit. Manuf.*, vol. 28, pp. 711–718, Aug. 2019, doi: 10.1016/j.addma.2019.06.019.
[22] S. W. Kang and J. Mueller, “Multiscale 3D printing via active nozzle size and shape control,” *Sci. Adv.*, vol. 10, no. 23, p. eadn7772, Jun. 2024, doi: 10.1126/sciadv.adn7772.
[23] R. O’Neill *et al.*, “Extent and mechanism of phase separation during the extrusion of calcium phosphate pastes,” *J. Mater. Sci.: Mater. Med.*, vol. 27, no. 2, p. 29, Feb. 2016, doi: 10.1007/s10856-015-5615-z.
[24] J. Jhun, D.-H. Lee, A. U. Rehman, S. Kang, and J.-H. Kim, “Development of a real-time geometric quality monitoring system for extruded filaments of 3D concrete printing construction,” *IEEE Access*, 2024, Accessed: Mar. 25, 2025. [Online]. Available: https://ieeexplore.ieee.org/abstract/document/10530624/
[25] F. Bos, R. Wolfs, Z. Ahmed, and T. Salet, “Additive manufacturing of concrete in construction: potentials and challenges of 3D concrete printing,” *Virtual Phys. Prototyp.*, vol. 11, no. 3, pp. 209–225, Jul. 2016, doi: 10.1080/17452759.2016.1209867.
[26] C. Joh, J. Lee, T. Q. Bui, J. Park, and I.-H. Yang, “Buildability and mechanical properties of 3D printed concrete,” *Materials*, vol. 13, no. 21, p. 4919, 2020.
[27] “3D Concrete Printing: A Systematic Review of Rheology, Mix Designs, Mechanical, Microstructural, and Durability Characteristics.” Accessed: Mar. 25, 2025. [Online]. Available: https://www.mdpi.com/1996-1944/14/14/3800
[28] Y. Zhou, F. Althoey, B. S. Alotaibi, Y. Gamil, and B. Iftikhar, “An overview of recent advancements in fibre-reinforced 3D printing concrete,” *Front. Mater.*, vol. 10, p. 1289340, Oct. 2023, doi: 10.3389/fmats.2023.1289340.
[29] A. Ramezani, S. Modaresi, P. Dashti, M. R. GivKashi, F. Moodi, and A. A. Ramezanianpour, “Effects of Different Types of Fibers on Fresh and Hardened Properties of Cement and Geopolymer-Based 3D Printed Mixtures: A Review,” *Buildings*, vol. 13, no. 4, Art. no. 4, Apr. 2023, doi: 10.3390/buildings13040945.
[30] W. Xu, D. Jiang, Q. Zhao, and L. Wang, “Study on printability of 3D printing carbon fiber reinforced eco-friendly concrete: Characterized by fluidity and consistency,” *Case Stud. Constr. Mater.*, vol. 21, p. e03589, Dec. 2024, doi: 10.1016/j.cscm.2024.e03589.